Carbohydrate Polymers 84 (2011) 1169–1175

Contents lists available at ScienceDirect

Carbohydrate Polymers

journal homepage: www.elsevier.com/locate/carbpol

Preparation of ethylenediamine-modified magnetic chitosan complex for adsorption of uranyl ions

Jing-song Wang[a,b,*], Rui-ting Peng[a,b], Jin-hui Yang[a,b], Yao-chi Liu[c], Xin-jiang Hu[d]

[a] School of Urban Construction, University of South China, Hengyang, Hunan 421001, China
[b] Key Discipline Laboratory of National Defence for Biotechnology in Uranium Mining and Hydrometallurgy, University of South China, Hengyang, Hunan 421001, China
[c] School of Chemistry and Chemical Engineering, Central South University, Changsha 410083, China
[d] College of Environmental Science and Engineering, Hunan University, Changsha 410082, China

ARTICLE INFO

Article history:
Received 25 November 2010
Received in revised form
30 December 2010
Accepted 5 January 2011
Available online 12 January 2011

Keywords:
Chitosan
Magnetic
Modified
Uranyl ions
Adsorption

ABSTRACT

Ethylenediamine-modified magnetic chitosan (EMMC) complex was developed as a novel magnetic adsorbent for the removal of uranyl ions. XRD spectrum indicated that the magnetic particles were pure Fe_3O_4 with a spinel structure, and the binding of chitosan did not result in a phase change. IR analysis demonstrated that Fe_3O_4 particles were successfully bounded by chitosan and more amino groups appeared in the EMMC samples. EMMC was found to be quite efficient to adsorb uranyl ions at pH 2–7. Equilibrium was established within 30 min, and the kinetic experimental data properly correlated with the pseudo-second-order kinetic model, indicating that the chemical sorption is the rate-limiting step. The adsorption data could be best interpreted by the Sips model with a maximum adsorption capacity of 82.83 mg U g^{-1}. The EMMC can be regenerated with high efficiency, suggesting that this adsorbent is satisfactory to reuse uranyl ions.

1. Introduction

A lot of polymer materials have been applied to separate metal ions. Attention has been focused on chitin, chitosan and its derivatives because they are abundant biopolymers and safe. Likewise, the presence of amino and hydroxyl groups give the polymers chelating properties that are very useful for metal uptake. In contrast to chitin, chitosan has superior adsorption ability for heavy metals due to its higher content of amino groups. Therefore, chitosan presents as a promising starting material for chelating resins (Kandile & Nasr, 2009). However, the solubility of chitosan in acid media and its light, soft properties are unfavorable. Chitosan can be modified chemically to prevent it from dissolution in acidic media or to enhance chelating capacity, or both, also can be prepared as composites. It is often crosslinked to confer better microbiological and mechanical resistance, but aldehyde-crosslinking may result in the loss of adsorption capacity because some amine groups are involved in the crosslinking reaction (Martinez et al., 2007). Several chemical regents, such as maleic anhydride (Guo et al., 2005), polydimethylsiloxane (Rutnakornpituk, Ngamdee, & Phinyocheep, 2006), glycine (Ramesh, Hasegawa, Sugimoto, Maki, & Ueda, 2008) and thiourea (Zhou, Wang, Liu, & Huang, 2009) have been demonstrated to be benefit to enhance the adsorption capacity of chitosan when used them to modify the polymer.

The application of magnetic carriers to solve some technical operations has received considerable attention in recent years. Magnetic properties could be imparted to adsorbents facilitating their trapping from the medium with the help of an external magnet. Recently, it was reported on the use of magnetic chitosan in removal of some metals from aqueous solutions (Monier, Ayad, Wei, & Sarhan, 2010; Zhou, Liu, Liu, & Huang, 2010; Muzzarelli, in press). It is noteworthy that these magnetic adsorbents have a high removal efficiency and fast adsorption rate due to the high specific surface area and the absence of internal diffusion resistance.

In this work, we developed an ethylenediamine-modified magnetic chitosan (EMMC) complex adsorbent using Fe_3O_4 nanoparticles as cores and chitosan as ionic exchange groups. The structure of the EMMC was confirmed using SEM, FTIR and XRD. The adsorption equilibrium and the kinetics of uranyl ions with this adsorbent were investigated to examine the potential application in uranium separation or analytical purposes.

* Corresponding author at: School of Urban Construction, University of South China, Hengyang, Hunan 421001, China. Tel.: +86 0734 8282394; fax: +86 0734 8282312.
E-mail address: xhwjs@163.com (J.-s. Wang).

0144-8617/$ – see front matter © 2011 Elsevier Ltd. All rights reserved.
doi:10.1016/j.carbpol.2011.01.007

2. Experimental

2.1. Materials

Chitosan with 90% acetylation degree and molecular weight of 1.5×10^5 was supplied by Sinopharm Chemical Reagent Co., Ltd. Glutaraldehyde and epichlorohydrin were provided by Tianjin Guangfu Fine Chemical Research Institute, Tianjin, China. Ethylenediamine was obtained from Changsha Sub-intersection Plastic Chemical Factory, Changsha, China. All reagents above were of Chemical grade. U_3O_8 was provided by the Key Discipline Laboratory of National Defence for Biotechnology in Uranium Mining and Hydrometallurgy, University of South China, China.

Uranium stock solution of 1000 mg L^{-1} was prepared by adding 0.1179 g of U_3O_8 into 5 mL of nitric acid then adding distilled water to 100 mL. The working solutions were prepared by appropriate dilution of the stock solutions immediately prior to their use. Solution pH was adjusted using 0.1 M HCl and NaOH solution.

2.2. Preparation of EMMC

Magnetic nanoparticles were prepared according to our previous study (Bao, Wang, Liu, & Liu, 2009). $FeCl_3$ and $FeSO_4$ were mixed in the solution with addition of sodium hydroxide to form Fe_3O_4 magnetic particles. The surfactant of Tween 80 and the ultrasonic generator were used to disperse the magnetic particles.

As reported in our previous study (Hu et al., 2010), EMMC was prepared by dissolving chitosan in acetic acid solution with stirring until completely dissolved and then the magnetic nanoparticles were added to the solution slowly at 50 °C. Glutaraldehyde and epichlorohydrin as cross-linking reagents with radio of 1/10 (w/w of crosslinker to chitosan) were used to form the gel, and ethylenediamine was introduced into the mixture to modify the chitosan beads.

2.3. Major equipment

A scanning electron microscope (Hatachi S-3000N, Japan), a FT-IR spectrophotometer (Thermo Nicolet IR200, USA), a dynamic laser light scattering apparatus (Winner 2005, China) and a D8 ADVANCE X-ray diffraction spectrometer (Bruker, German) were employed to confirm the structure and morphology of EMMC samples.

2.4. Adsorption and elusion

The adsorption and elusion experiments were conducted in a batch system. The concentration of the UO_2^{2+} (based on uranium, mg L^{-1}) was analyzed by spectrophotometric arsenazo III method using a UV–vis spectrophotometer at 578 nm. Each of the experiment was repeated thrice and the average values were obtained.

The percentage removal (η) and the amount of UO_2^{2+} adsorbed by the adsorbent was calculated according to following equations:

$$\eta\% = \frac{C_0 - C}{C_0} \times 100 \quad (1)$$

$$q_e = \frac{(C_0 - C_{eq})V}{M} \quad (2)$$

where q_e is the equilibrium adsorption capacity per gram dry weight of the adsorbents, mg g^{-1}; C_0 is the initial concentration of UO_2^{2+} in the solution, mg L^{-1}; C_{eq} is the final or equilibrium concentration of the UO_2^{2+} after adsorption, mg L^{-1}; V is the volume of the aqueous solution, L; and M is the amount of adsorbents, g.

After adsorption, the EMMC particles were separated from the solution by applying a magnetic field, then added into the eluent (NaOH) and stirred at 250 rpm for 20 min at 303 K. After each cycle of recovery, the adsorbent was washed with distilled water and used in the succeeding cycle.

The desorption ratio (D%) was calculated by

$$D\% = \frac{W_d}{W_a} \times 100 \quad (3)$$

where W_d is the amount of uranium (mg) in the desorption medium and W_a is the amount of uranium (mg) adsorbed on EMMC.

3. Results and discussion

3.1. Characterization of EMMC

The SEM micrograph of EMMC is given in Fig. 1. The synthesized EMMC had an approximate spherical shape with a mean diameter of about 80 μm. The images illustrate that the EMMC particles have holes and some small openings on the surface, which increases the contact area and can improve metal ion adsorption.

The EDS spectrum (Fig. 1a) of EMMC before adsorption shows that the three major constituents, i.e., C, O and Fe of chitosan and Fe_3O_4. The EDS spectrum (Fig. 1b) of EMMC after adsorption of UO_2^{2+} presented a new appearing peak at 3.2 keV, which is associated to U element. This provided an evidence for UO_2^{2+} adsorption onto EMMC surface.

Fig. 2 shows XRD spectrum of Fe_3O_4 particles and EMMC. Six characteristic peaks for Fe_3O_4 (2θ = 30.1, 35.4, 43.0, 53.5, 57.0 and 62.5) marked by their indices [(2 2 0), (3 1 1), (4 0 0), (4 2 2), (5 1 1), and (4 4 0)] were observed for both samples. These peaks are consistent with the database in JCPDS file (PDF No. 65-3107) and reveal that the resultant magnetic particles were pure Fe_3O_4 with a spinel structure (Li, Jiang, Huang, & Jie Chen, 2008; Tran, Tran, & Nguyen, 2010). As compared with Fe_3O_4 particles, the characteristic peaks in XRD patterns of EMMC shifted slightly to lower angles, indicating that the interaction between chitosan and Fe_3O_4 particles has occurred.

FTIR spectra of the chitosan and EMMC are shown in Fig. 3. The bands at 560–660 cm^{-1} are associated with the metal–O stretching vibration. The adsorption band around 3420 cm^{-1} reveals the stretching vibration of N–H group bonded with O–H group in chitosan, and at around 1650 cm^{-1} confirms the N–H scissoring from the primary amine, due to the free amino groups in the crosslinked chitosan (Kawamura, Yoshida, Asai, & Tanibe, 1998). The bands at 1450 cm^{-1}, 1389 and 1076 cm^{-1} are related to amide II, C–O group and O–H group. The increasing intensity at 1450 cm^{-1} in the spectrum of EMMC indicated that EMMC has more amine groups than chitosan. Finally, it can be seen that all the characteristic bands are similar for both chitosan and EMMC.

Size distribution of Fe_3O_4 and EMMC particles is presented in Fig. 4. The size of Fe_3O_4 was in the range from 0.1 μm to 10 μm, the mean diameter was 1.1 μm. The size of EMMC particles was in the range from 10 μm to 500 μm, the mean diameter was 96 μm, which was consistent with the result of the SEM measurement.

3.2. Adsorption behavior of UO_2^{2+}

The effect of pH on the adsorption of UO_2^{2+} by EMMC at 303 K and an initial concentration of 10 mg L^{-1} is illustrated in Fig. 5(a). The EMMC adsorbent can adsorb UO_2^{2+} quite efficiently in the pH range of 2.0–7.0. However, the observed decline of adsorption capacity at pH > 7.0 is attributed to the precipitation of uranium, and the lower uptake at pH < 2.0 may be attributed to the partial protonation of the active groups and the competition of H^+ with UO_2^{2+} for adsorption sites on EMMC. The pH value plays an important role in the adsorption of UO_2^{2+} onto EMMC, because the pH of the solution can influence the aqueous chemistry of uranium and the properties of functional groups of adsorbent. EMMC

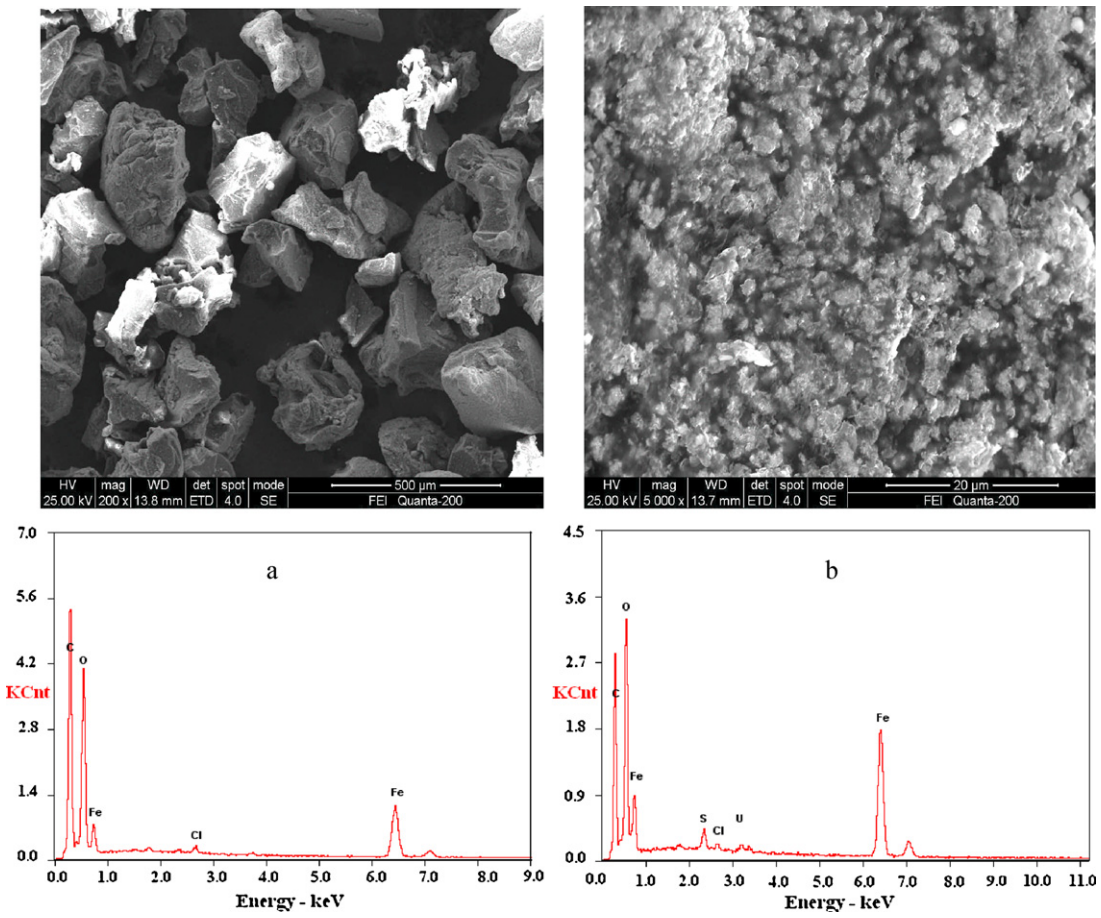

Fig. 1. SEM photographs and EDS spectra of EMMC. (a) Before adsorption, (b) after adsorption.

might adsorb the species of UO_2^{2+} by forming the stable chelates with functional moieties introduced to it. The maximum adsorption capacity occurred at pH 3.0, and similar results (data not shown) were obtained for initial UO_2^{2+} concentration of 50 mg L^{-1} and 100 mg L^{-1}, so the following adsorption studies were carried out at this pH value.

The effect of adsorbent dose on UO_2^{2+} adsorption is presented in Fig. 5(b). Maximum removal efficiency is attained at dose of 2 g L^{-1} and becomes constant thereafter. This trend could be explained as a consequence of a partial aggregation of adsorbent at higher concentrations, which results in less binding sites for metal ions available and decreases effective surface area for the adsorption. Furthermore, the adsorption capacity of EMMC declines with the increase of adsorbent dose, which indicates that the adsorption sites remain unsaturated. Therefore, for 10 mg L^{-1} UO_2^{2+} solution, 2 g L^{-1} adsorbent dose was selected for further experiments. For 50 mg L^{-1} and 100 mg L^{-1} UO_2^{2+} solution, the experiment was conducted as above, and 5 g L^{-1} is the optimum adsorbent dose.

The percentage removal and adsorption capacity at different UO_2^{2+} concentrations are presented in Fig. 5(c). Maximum adsorption capacity was observed at the initial UO_2^{2+} concentration of 600 mg L^{-1}. Maximum removal efficiency was attained to 99.8% at

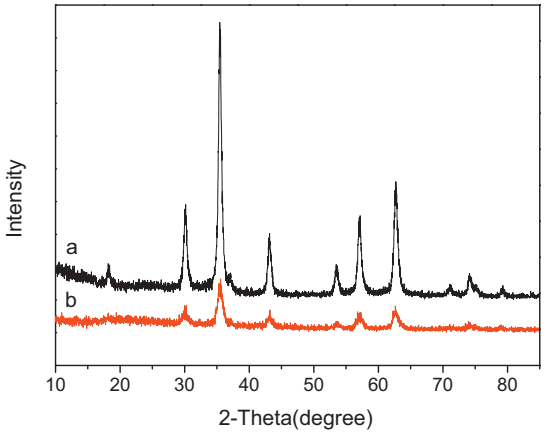

Fig. 2. XRD spectrum of (a) Fe_3O_4 particles, (b) EMMC.

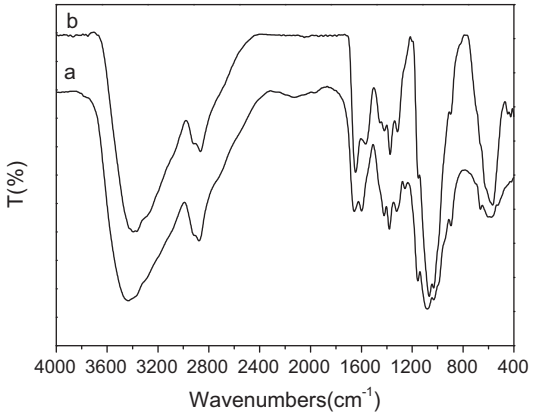

Fig. 3. IR spectra of (a) chitosan, (b) EMMC.

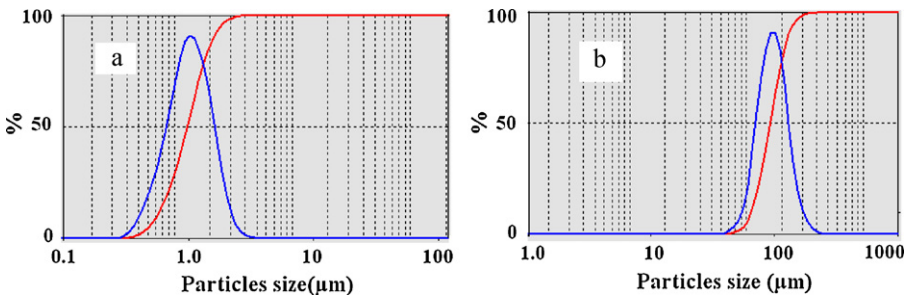

Fig. 4. Particles size distribution of (a) Fe_3O_4 particles, (b) EMMC.

the initial UO_2^{2+} concentration of 10 mg L^{-1}. In the initial concentration range of 10–200 mg L^{-1}, the removal efficiency is higher than 90%, indicating that EMMC adsorbent is quiet efficient in UO_2^{2+} adsorption.

The influence of temperature on UO_2^{2+} adsorption is shown in Fig. 5(d). For all the temperatures studied, the equilibrium was attained within 30 min, and when the temperature of the solution increased from 293 to 313 K, the removal decreased. The results show that the UO_2^{2+} adsorption on EMMC is an exothermic process. The exothermic nature of adsorption has also been reported for U(VI) adsorption on *Cystoseria indica* algae (Khani, Keshtkar, Ghannadi, & Pahlavanzadeh, 2008) and sepiolite (Donat, 2009), Hg(II) adsorption on EMCR (Zhou et al., 2010). However, the studies of U(VI) adsorption on PGTFS–COOH (Anirudhan & Radhakrishnan, 2009) and on GMA (Donia, Atia, Moussa, El-Sherif, & Abd El-Magied, 2009), Cu(II) adsorption on α-KA-CCMNPs (Zhou, Branford-White, Nie, & Zhu, 2009) reported the endothermic nature of the adsorption process.

The change of UO_2^{2+} uptake by EMMC as a function of contact time is plotted and presented in Fig. 6(a). It can be seen that the UO_2^{2+} uptake reached a maximum at 15 min with initial UO_2^{2+} concentration of 10 and 50 mg L^{-1}, and at 30 min with initial UO_2^{2+} concentration of 100 mg L^{-1}. In general, about 99% of the total metal ions adsorption was achieved within 30 min and remained constant up to 60 min. Therefore, 30 min was considered sufficient to establish equilibrium.

3.3. Kinetic studies

In order to evaluate the kinetic mechanism that controls the adsorption process, pseudo-first-order, pseudo-second-order, and intra-particle diffusion models were employed to interpret the

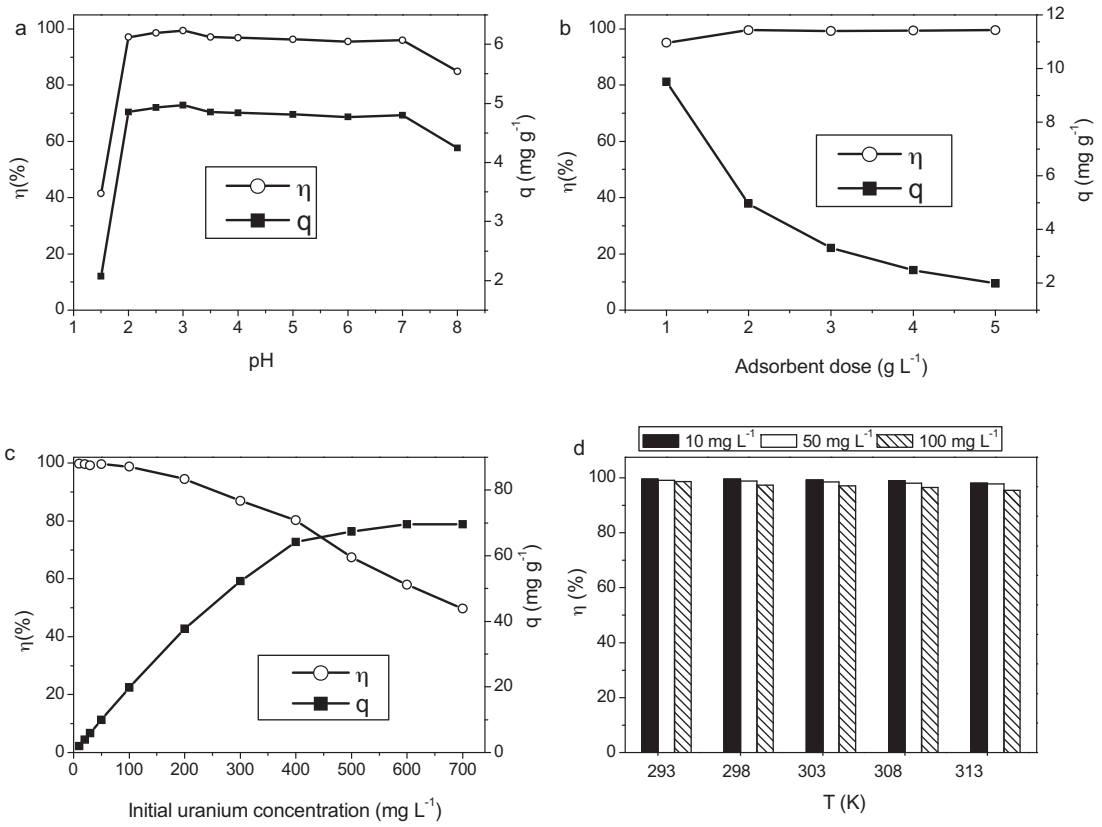

Fig. 5. Adsorption of UO_2^{2+} on EMMC at different. (a) pH (conditions: adsorbent dose = 2 g L^{-1}; UO_2^{2+} = 10 mg L^{-1}; contact time = 30 min; temperature = 303 K; agitation speed = 250 rpm), (b) adsorbent dose (conditions: pH 3; UO_2^{2+} = 10 mg L^{-1}; contact time = 30 min; temperature = 303 K; agitation speed = 250 rpm), (c) initial UO_2^{2+} concentration (conditions: pH 3; adsorbent dose = 5 g L^{-1}; contact time = 30 min; temperature = 303 K; agitation speed = 250 rpm), (d) temperature (conditions: pH 3; adsorbent dose = 5 g L^{-1}; contact time = 30 min; agitation speed = 250 rpm).

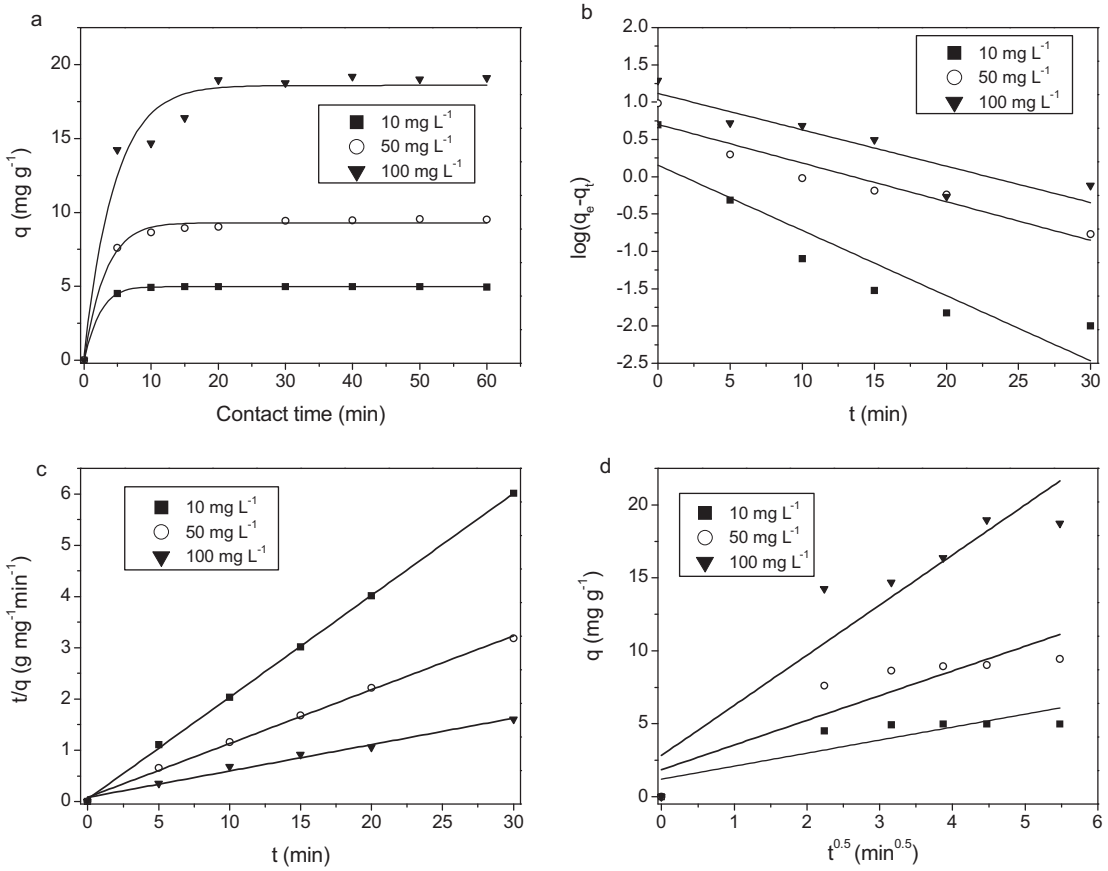

Fig. 6. (a) Adsorption of UO_2^{2+} on EMMC at different contact time and plot of (b) the pseudo-first order equation, (c) the pseudo-second order equation, (d) the intra-particle diffusion equation for the adsorption of UO_2^{2+} on EMMC (conditions: pH 3; for 10 mg L^{-1} UO_2^{2+}, adsorbent dose = 2 g L^{-1}, others, adsorbent dose = 5 g L^{-1}; temperature = 303 K; agitation speed = 250 rpm).

experimental data. A good correlation of the kinetic data can explain the adsorption mechanism of the metal ions on the solid phase (Wu, Tseng, & Juang, 2001).

The linear form of the pseudo-first-order rate equation by Lagergren is given as

$$\log(q_e - q_t) = \log q_e - \frac{k_1}{2.303}t \quad (4)$$

where q_e and q_t are the amounts of adsorbed UO_2^{2+} on the adsorbent at equilibrium and at time t, respectively (mg g^{-1}), and k_1 is the first-order adsorption rate constant (min^{-1}).

The linear form of the pseudo-second-order model is represented as

$$\frac{t}{q_t} = \frac{1}{k_2 q_e^2} + \frac{1}{q_e}t \quad (5)$$

where k_2 is the second-order adsorption rate constant (g mg^{-1} min^{-1}), and q_e is the adsorption capacity calculated by the pseudo-second-order kinetic model (mg g^{-1}).

The initial adsorption rate h (mg g^{-1} min^{-1}) can be calculated from k_2 and q_e using

$$h = k_2 q_e^2 \quad (6)$$

The intra-particle diffusion model is expressed as

$$q_t = k_p t^{1/2} + C \quad (7)$$

where k_p is the intra-particle diffusion rate constant (mg g^{-1} $min^{-0.5}$) and C of adsorption constant is the intercept.

The regress data fit the three kinetic models are shown in Fig. 6(b)–(d). The correlation coefficients for the pseudo-first-order equation obtained at all the studied concentrations range between 0.785 and 0.879, and the theoretical q_e values calculated from the pseudo-first-order equation are not in agreement of the experimental data, suggesting that this adsorption system is not a first-order reaction. Also low coefficients range between 0.666 and 0.840 with intra-particle diffusion model, suggesting that intra-particle diffusion is not the rate-controlling step. High correlation coefficients are obtained ($R^2 > 0.982$) when employing the pseudo-second-order model for all concentrations and the calculating equilibrium adsorption capacity is close to the experimental data. This indicates that the pseudo-second-order model can be applied to predict the adsorption kinetic and suggests chemisorption as the rate-controlling step involving valence forces through sharing or exchange of electrons between the adsorbent surface and adsorbate ions and no involvement of a mass transfer in solution (Ho, McKay, Wase, & Forster, 2000; Yurdakoc, Scki, & Yuedakoc, 2005).

In fact, most adsorption reactions take place through multistep mechanism comprising (i) external film diffusion, (ii) intra-particle diffusion and (iii) interaction between adsorbate and active site. In this case, the first step is excluded by agitating the solution at a high speed. Due to loosen and porous internal structure of the adsorbent (Fig. 1), UO_2^{2+} can diffuse easily to the inner surface, also indicating that intra-particle diffusion is not a rate-limiting step. Therefore, the third step controls the adsorption rate. Furthermore, EMMC is characterized by high percentage of nitrogen and oxygen, present in the form of amine and hydroxyl groups that are responsible for metal ion binding through chelation mechanisms. Amine sites are the main reactive groups for metal ions though hydroxyl groups, especially in the C-3 position, and they may contribute to adsorption (Varma, Deshpande, & Kennedy, 2004).

3.4. Adsorption isotherms

In this study, the adsorption isotherms were investigated using four equilibrium models, which are Langmuir, Freundlich, Temkin and Sips isotherm models.

The Langmuir equation assumes that (Parab et al., 2005): (i) the solid surface presents a finite number of identical sites which are energetically uniform; (ii) there is no interactions between adsorbed species, meaning that the amount adsorbed has no influence on the rate of adsorption and (iii) a monolayer is formed when the solid surface reaches saturation. This model is expressed as

$$q = \frac{q_m K_L C_e}{1 + K_L C_e} \tag{8}$$

where C_e is the concentration of the adsorbate in solution at equilibrium (mg L^{-1}), q_e is the adsorption capacity at equilibrium (mg g^{-1}), q_m is the maximum adsorption capacity of the adsorbent (mg g^{-1}), and K_L is the Langmuir adsorption constant related to the energy of adsorption (L mg^{-1}).

The Freundlich model assumes a heterogeneous adsorption surface and active sites with different energy. The Freundlich model is represented as

$$q = k_F C_e^{1/n} \tag{9}$$

where K_F is a constant relating the adsorption capacity (L g^{-1}), and $1/n$ is an empirical parameter relating the adsorption intensity, which varies with the heterogeneity of the material.

To resolve the problem of continuing increase in the adsorbed amount with a rising concentration as observed for Freundlich model, an expression was proposed as Sips isotherm model, differing only on the finite limit of adsorbed amount at sufficiently high concentration. It is given as

$$q = \frac{q_m K_{eq} C_e^n}{1 + K_{eq} C_e^n} \tag{10}$$

where K_{eq} represents the equilibrium constant of the Sips equation (L mg^{-1}), and q_m is the maximum adsorption capacity (mg g^{-1}). The parameter n is regarded as the parameter characterizing the system's heterogeneity, which could stem from the adsorbent or the metal, or a combination of both. If n is unit, the Sips isotherm equation turns to the Langmuir equation and it implies a homogeneous adsorption process.

The Temkin isotherm takes into account the interactions between adsorbents and metal ions to be adsorbed and is based on the assumption that the free energy of adsorption is a function of the surface coverage. The isotherm model is written as

$$q_e = \frac{RT}{b_T} \ln(a_T C_e) \tag{11}$$

where a_T is the equilibrium binding constant corresponding to the maximum binding energy, b_T is the Temkin isotherm constant, T is the temperature (K), and R is the ideal gas constant (8.314 J mol^{-1} K^{-1}).

Fig. 7 shows the equilibrium adsorption of UO_2^{2+} onto the EMMC and the fitting plot of the four isotherm models. For the studied system, the Sips isotherm correlates best (R^2 = 0.994) with the experimental data from adsorption equilibrium of UO_2^{2+} by EMMC in these four models, suggesting the heterogeneity of the adsorption, which may be attributed to the complicated form of UO_2^{2+} at the acid pH regions and the heterogeneous distribution of the active sites on EMMC surface. Other studies (Apiratikul & Pavasant, 2008; Senthilkumar, Vijayaraghavan, Thilakavathi, Iyer, & Velan, 2007; Vijayaraghavan, Padmesh, Palanivelu, & Velan, 2006) also reported the high value of coefficient correlation when using Sips isotherm model to predict heavy metal adsorption experimental results. The

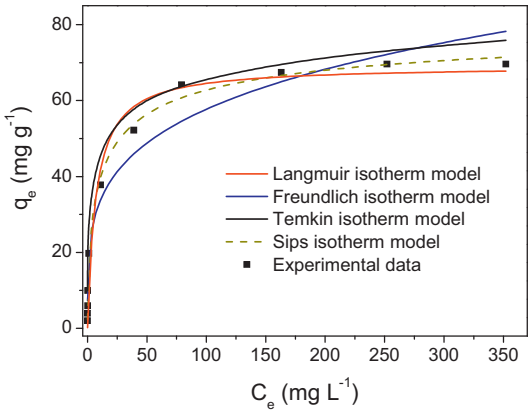

Fig. 7. Plots of q_e vs. C_e for the adsorption of UO_2^{2+} onto EMMC at pH 3 and 303 K.

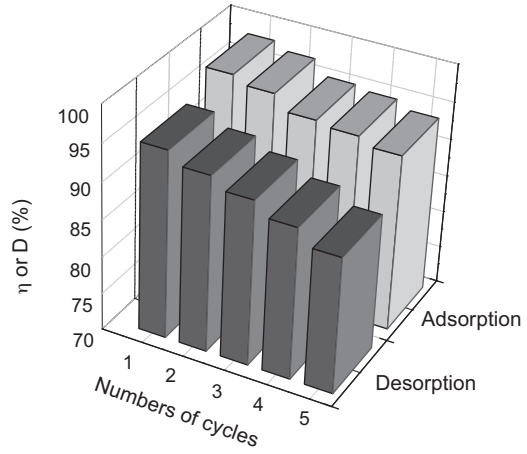

Fig. 8. Repetitive adsorption and desorption ratio for UO_2^{2+} (conditions: adsorbent dose, 5.0 g L^{-1}; temperature, 303 K; agitation speed, 250 rpm).

maximum adsorption capacity of EMMC for UO_2^{2+} obtained by Sips isotherm model is 82.83 mg U g^{-1}.

3.5. Elution and reuse

NaOH was selected as the eluent based on economics consideration. Less than 2% increase of desorption ratio with the increase of eluent concentration from 0.1 to 0.5 M, so the concentration was determined to be 0.1 M for further study. In order to obtain the reusability of EMMC, adsorption–desorption cycles were repeated five times by using the same adsorbent in a batch experimental. The results are shown in Fig. 8. It can be observed only 4.5% loss of the adsorption capacity and 7% loss of desorption ratio after five circles of regeneration, suggesting that this adsorbent is satisfactory to reuse UO_2^{2+} from water.

4. Conclusion

The ethylenediamine-modified magnetic chitosan (EMMC) complex adsorbent was favorable to collect UO_2^{2+} from aqueous solution. The removal efficiency of UO_2^{2+} by EMMC was high in a wide pH (2–7) range and initial UO_2^{2+} concentration range (10–200 mg L^{-1}). Likewise, the adsorption capacity of EMMC has superior over some reported adsorbents for uranium (Oshita et al., 2008; Wang, Liu, Wang, Xie, & Deng, 2009;). The uptake of UO_2^{2+} by EMMC was quite rapid and the experimental data obeyed the pseudo-second-order model, indicating that the chemical sorption is the rate-limiting step. The equilibrium data fitted well to Sips

isotherm model. A little decrease in the adsorption capacity and desorption ratio were achieved after five regeneration cycles, indicating that the adsorbent was suitable to regenerate and reuse UO_2^{2+}.

Acknowledgements

The authors would like to thank financial support from the National Natural Science Foundation of China (Nos. 20707008, 51074192), the Scientific Research Fund of Hunan Provincial Education Department (No. 06B082) and the Construct Program of the Key Discipline in Hunan Province.

References

Apiratikul, R., & Pavasant, P. (2008). Batch and column studies of biosorption of heavy metals by *Caulerpa lentillifera*. *Bioresource Technology*, *99*, 2766–2777.

Anirudhan, T. S., & Radhakrishnan, P. G. (2009). Kinetics, thermodynamics and surface heterogeneity assessment of uranium(VI) adsorption onto cation exchange resin derived from a lignocellulosic residue. *Applied Surface Science*, *255*, 4983–4991.

Bao, Z. L., Wang, J. S., Liu, H. J., & Liu, L. P. (2009). Preparation of water-based Fe_3O_4 magnetic fluids via chemical co-precipitation as precursors of complex adsorbent. In *2009 International Symposium on Environmental Science and Technology, vol. 2(part B)* (pp. 1585–1591).

Donat, R. (2009). The removal of uranium (VI) from aqueous solutions onto natural sepiolite. *Journal of Chemical Thermodynamics*, *41*, 829–835.

Donia, A. M., Atia, A. A., Moussa, E. M. M., El-Sherif, A. M., & Abd El-Magied, M. O. (2009). Removal of uranium(VI) from aqueous solutions using glycidyl methacrylate chelating resins. *Hydrometallurgy*, *95*, 183–189.

Guo, T. Y., Xia, Y. Q., Hao, G. J., Zhang, B. H., Fu, G. Q., Yuan, Z., et al. (2005). Chemically modified chitosan beads as matrices for adsorptive separation of proteins by molecularly imprinted polymer. *Carbohydrate Polymers*, *62*, 214–221.

Hu, X. J., Wang, J. S., Liu, Y. G., Li, X., Zeng, G. M., Bao, Z. L., et al. (2010). Adsorption of chromium (VI) by ethylenediamine-modified cross-linked magnetic chitosan resin: Isotherms, kinetics and thermodynamics. *Journal of Hazardous Materials*, *185*, 306–314.

Ho, Y. S, McKay, G., Wase, D. A. J., & Forster, C. F. (2000). Study of the sorption of divalent metal ions on to peat. *Adsorption Science and Technology*, *18*, 639–650.

Kandile, N. G., & Nasr, A. S. (2009). Environment friendly modified chitosan hydrogels as a matrix for adsorption of metal ions, synthesis and characterization. *Carbohydrate Polymers*, *78*, 753–759.

Kawamura, Y., Yoshida, H., Asai, S., & Tanibe, H. (1998). Recovery of $HgCl_2$ using polyaminated highly porous chitosan beads-effect of salt and acid. *Journal of Chemical Engineering of Japan*, *31*, 1–6.

Khani, M. H., Keshtkar, A. R., Ghannadi, M., & Pahlavanzadeh, H. (2008). Equilibrium, kinetic and thermodynamic study of the biosorption of uranium onto *Cystoseria indica* algae. *Journal of Hazardous Materials*, *150*, 612–618.

Li, G. Y, Jiang, Y. R., Huang, K. L., Ding, & Jie Chen, J. (2008). Preparation and properties of magnetic Fe_3O_4–chitosan nanoparticles. *Journal of Alloys and Compounds*, *466*, 451–456.

Martinez, L., Agnely, F., Leclerc, B., Siepmann, J., Cotte, M., Deiger, S., et al. (2007). Cross-linking of chitosan and chitosan poly(ethylene oxide) beads: A theoretical treatment. *European Journal of Pharmaceutics and Biopharmaceutics*, *67*, 339–348.

Muzzarelli, R. A. A. Potential of chitin/chitosan-bearing materials for uranium recovery: An interdisciplinary review. *Carbohydrate Polymers*, in press, doi:10.1016/j.carbpol.2010.12.025.

Monier, M., Ayad, D. M., Wei, Y., & Sarhan, A. A. (2010). Adsorption of Cu(II), Co(II), and Ni(II) ions by modified magnetic chitosan chelating resin. *Journal of Hazardous Materials*, *77*, 962–970.

Oshita, K, Seo, K., Akhmad Sabarudin, A., Oshima, M., Takayanagi, T., & Motomizu, S. (2008). Synthesis of chitosan resin possessing a phenylarsonic acid moiety for collection concentration of uranium and its determination by ICP-AES. *Analytical and Bioanalytical Chemistry*, *390*, 1927–1932.

Parab, H., Joshi, S., Shenoy, N., Verma, R., Lali, A., & Sudersanan, M. (2005). Uranium removal from aqueous solution by coir pith: Equilibrium and kinetic studies. *Bioresource Technology*, *96*, 1241–1248.

Ramesh, A., Hasegawa, H., Sugimoto, W., Maki, T., & Ueda, K. (2008). Adsorption of gold(III), platinum(IV) and palladium(II) onto glycine modified crosslinked chitosan resin. *Bioresource Technology*, *99*, 3801–3809.

Rutnakornpituk, M., Ngamdee, P., & Phinyocheep, P. (2006). Preparation and properties of polydimethylsiloxane-modified chitosan. *Carbohydrate Polymers*, *63*, 229–237.

Senthilkumar, R., Vijayaraghavan, K., Thilakavathi, M., Iyer, P. V. R., & Velan, M. (2007). Application of seaweeds for the removal of lead from aqueous solution. *Biochemical Engineering Journal*, *33*, 211–216.

Tran, H. V., Tran, L. D., & Nguyen, T. N. (2010). Preparation of chitosan/magnetite composite beads and their application for removal of Pb(II) and Ni(II) from aqueous solution. *Materials Science and Engineering*, *C30*, 304–310.

Varma, A. J., Deshpande, S. V., & Kennedy, J. F. (2004). Metal complexation by chitosan and its derivatives: A review. *Carbohydrate Polymers*, *55*, 77–93.

Vijayaraghavan, K., Padmesh, T. V. N., Palanivelu, K., & Velan, M. (2006). Biosorption of nickel(II) ions onto *Sargassum wightii*: Application of two-parameter and three-parameter isotherm models. *Journal of Hazardous Materials*, *B133*, 304–308.

Wang, G., Liu, J., Wang, X., Xie, Z., & Deng, N. (2009). Adsorption of uranium (VI) from aqueous solution onto cross-linked chitosan. *Journal of Hazardous Materials*, *168*, 1053–1058.

Wu, F. C., Tseng, R. L., & Juang, R. S. (2001). Kinetic modeling of liquid-phase adsorption of reactive dyes and metal ions on chitosan. *Water Research*, *35*, 613–618.

Yurdakoc, M., Scki, Y., & Yuedakoc, S. K. (2005). Kinetic and thermodynamic studies of boron removal by Siral 5, Siral 40, and Srial 80. *Journal of Colloid and Interface Science*, *286*, 440–446.

Zhou, L, Wang, Y., Liu, Z., & Huang, Q. (2009). Characteristics of equilibrium, kinetics studies for adsorption of Hg(II), Cu(II), and Ni(II) ions by thiourea-modified magnetic chitosan microspheres. *Journal of Hazardous Materials*, *161*, 995–1002.

Zhou, L. M., Liu, Z. R., Liu, J. H., & Huang, Q. W. (2010). Adsorption of Hg(II) from aqueous solution by ethylenediamine-modified magnetic crosslinking chitosan microspheres. *Desalination*, *258*, 41–47.

Zhou, Y. T., Branford-White, C., Nie, H. L., & Zhu, L. M. (2009). Adsorption mechanism of Cu^{2+} from aqueous solution by chitosan-coated magnetic nanoparticles modified with α-ketoglutaric acid. *Colloids and Surfaces B: Biointerfaces*, *74*, 244–252.